On Martian nitrogen dayglow emission observed by SPICAM UV spectrograph/Mars Express

François Leblanc, Jean-Yves Chaufray, Jean-Loup Bertaux

On Martian nitrogen dayglow emission observed by SPICAM UV spectrograph/Mars Express

F. Leblanc,[1,2] J. Y. Chaufray,[1] and J. L. Bertaux[1]

Received 12 October 2006; revised 18 December 2006; accepted 21 December 2006; published 27 January 2007.

[1] SPICAM UV spectrograph on board Mars Express has reported, for the first time, the identification of the N_2 VK (0,5) and (0,6) band emissions in the Martian dayglow. The derived exospheric temperature of the N_2 species in the upper Martian atmosphere is equal to 190 ± 51 K for areocentric longitudes between 100° and 171° and equal to 257 ± 71 K for areocentric longitudes between 287° and 321°. These temperatures are in agreement with the ones deduced from the analysis of the 289 nm emission associated with the CO_2 major Martian atmospheric species. The intensity of the N_2 VK (0,6) band is found to be ~3 times smaller than the calculated intensity of Fox and Dalgarno (1979) which is reasonable when considering the uncertainties in the parameters used by Fox and Dalgarno (1979) and the uncertainties on SPICAM UVS observations. **Citation:** Leblanc, F., J. Y. Chaufray, and J. L. Bertaux (2007), On Martian nitrogen dayglow emission observed by SPICAM UV spectrograph/Mars Express, *Geophys. Res. Lett.*, *34*, L02206, doi:10.1029/2006GL028437.

1. Introduction

[2] SPICAM light on board Mars Express is a spectrograph composed of UV (110–300 nm) and IR (1 to 1.7 μm) channels [*Bertaux et al.*, 2006]. Since January 2004, SPICAM UV spectrograph (SPICAM UVS) has regularly observed the Martian upper atmosphere and measured its airglow emissions. The observations by SPICAM UVS of the Martian dayglow have been published by *Leblanc et al.* [2006], where the first observation of the N_2 Vegard Kaplan (0,5) and (0,6) band emissions have been reported.

[3] The non-detection of the N_2 Vegard Kaplan (VK) band emission in the Martian upper atmosphere [*Barth et al.*, 1969] has been discussed after Mariner 6, 7 and 9 missions by *Dalgarno and McElroy* [1970]. These authors concluded that the mixing ratio of the N_2 in the CO_2 Martian atmosphere should not exceed 5% in a uniformly mixed atmosphere.

[4] Later, *Fox and Dalgarno* [1979] published a complete calculation of the Martian dayglow emissions in the UV range, including the emission associated with the N_2 species [see also *Fox et al.*, 1977]. These authors asserted that the main pathway to produce the $A^3\Sigma_u^+$ excited state of the VK band system is by electron impact. The transition from this excited state to the N_2 fundamental state $X^1\Sigma_g^+$ may then lead to emission, in particular, at 260.4 nm associated with the VK (0,5) band and at 276.2 nm associated with the VK (0,6) band. On Earth, the $A^3\Sigma_u^+$ state is efficiently quenched by O and O_2, whereas CO_2, which is the major constituent of the Martian atmosphere, is less efficient at quenching this excited state [*Meyer et al.*, 1969; *Young et al.*, 1969; *Dreyer et al.*, 1974]. As a consequence, emissions associated with the VK band system with an intensity within the sensitivity of SPICAM UVS has been predicted in the Martian upper atmosphere [*Fox and Dalgarno*, 1979]. The observation by SPICAM UVS of the emissions associated to two bands of the VK system confirms this prediction made 30 years earlier. Moreover, SPICAM UVS measured intensities of the (0,5) and (0,6) bands, that are in agreement within a factor ~3 with the *Fox and Dalgarno* [1979] calculation.

[5] We here describe the whole set of observations of the N_2 emission in the Martian upper atmosphere. Section 2 describes the data set. Section 3 provides an analysis of the measured N_2 emissions and section 4 summarizes its main characteristics.

2. Data Set

[6] *Leblanc et al.* [2006] analyzed the first part of the present set of observations of the Martian dayglow between Mars Express orbit 947 and orbit 1457. In this paper we use the whole set of available observations that is up to May 2006 (orbit 2967). We display in Table 1 the only orbits during which an identification (at least with a signal to noise ratio larger than one) of the VK (0,5) or (0,6) band emissions was possible. With respect to the coverage described by *Leblanc et al.* [2006], this new set essentially extends the number of observations made at large areocentric longitude (Ls).

[7] The method used to derive N_2 emission intensity from SPICAM observations has been described by *Leblanc et al.* [2006]. It consists of a direct integration of the line between two predefined wavelengths from which is subtracted a background emission estimated from the part of the spectrum close to the wavelength ranges of the integrated emission. The uncertainty is calculated from the theoretical instrumental uncertainty. The absolute calibration is obtained by the observation of selected calibrated stars [*Bertaux et al.*, 2006].

3. Analysis

[8] As described by *Leblanc et al.* [2006], only two emission bands of the N_2 VK system can be identified with a signal/noise ratio larger than one. The other bands cannot be identified because they are overlapped with stronger dayglow emission. In particular, there is only a partial

[1]Service d'Aéronomie, Centre National de la Recherche Scientifique, Institut Pierre-Simon Laplace, Verrières-le-Buisson, France.
[2]Now at Osservatorio Astronomico di Trieste, Trieste, Italy.

0094-8276/07/2006GL028437

Table 1. SPICAM Observation Set of the Martian Dayglow[a]

Date	Orbit	Bin Size	Ls	F10.7	Latitude	Longitude	SZA	Altitude
2004 10 15	947	32	100.9	33	28N–6S–41S	114–124–137	28–52–86	392–77–370
2004 10 15	948	32	101.1	33	28N–5S–41S	16–26–40	27–52–86	380–77–373
2004 10 16	952	32	101.6	33.6	28N–4S–40S	343–353–6	27–51–85	387–78–372
2004 10 17	958	32	102.3	33.7	11N–4S–39S	119–124–137	37–49–84	131–76–374
2004 10 18	959	32	102.4	34.2	30N–4S–39S	15–25–38	26–49–83	392–77–370
2004 10 24	981	32	105.2	32.7	34N–0S–35S	11–23–36	22–44–78	398–75–367
2004 10 24	983	32	105.5	32.7	33N–0S–35S	175–187–200	22–43–78	395–77–369
2004 12 16	1172	16	130.1	35.6	61N–25N–15S	30–17–9	58–45–54	402–76–486
2005 01 03	1234	32	138.6	37.9	70N–34N–5N	72–46–38	65–40–34	412–80–303
2005 01 12	1267	16	143.2	38.9	73N–40N–1N	84–45–32	71–41–29	414–81–477
2005 01 13	1271	16	143.7	36.4	74N–40N–25S	52–12–351	71–40–44	420–81–1312
2005 01 17	1285	16	145.7	36.5	75N–43N–4N	124–76–63	74–41–25	418–82–476
2005 01 21	1298	16	147.5	48.5	75N–45N–6N	296–240–225	76–42–22	414–83–480
2005 01 27	1321	16	151	56.2	75N–48N–11N	212–141–124	80–45–17	421–85–474
2005 02 04	1349	16	154.9	36.5	74N–40N–8N	264–267–266	65–38–28	305–79–336
2005 02 04	1350	16	155	36.5	68N–35N–5N	159–169–171	59–35–32	266–76–315
2005 02 10	1371	16	158	36	72N–56N–19N	6–272–250	90–53–14	419–87–478
2005 02 22	1413	16	164	53.9	67N–62N–26N	213–109–82	98–59–20	429–89–470
2005 02 22	1414	16	164	53.9	67N–62N–26N	114–12–343	98–60–20	423–89–476
2005 02 26	1426	16	166	44	65N–64N–29N	19–275–244	100–62–23	434–90–464
2005 03 06	1457	16	171	34	61N–67N–34N	218–116–78	106–68–30	441–91–460
2005 09 13	2137	16	287.2	59.8.	55S–21S–10N	331–359–13	35–7–41	459–67–342
2005 09 17	2151	16	289.6	56.4	57S–29S–6N	143–111–91	65–45–44	346–69–374
2005 09 22	2166	16	292	51.4	59S–22S–12N	8–31–40	39–2–38	471–67–390
2005 10 17	2259	16	307.7	38.1	55S–17S–13N	266–249–240	35–17–41	316–82–319
2005 10 18	2260	16	307.9	38.7	57S–2(S–14N	188–199–205	39–27–49	290–82–468
2005 10 30	2304	32	315	34.1	55S–19S–9N	164–145–136	39–28–44	275–83–289
2005 11 06	2329	32	319	36.2	73S–43S–8S	148–210–221	77–41–22	462–85–428
2005 11 10	2342	32	321.1	37.2	52S–56S–33S	293–354–33	96–59–23	367–80–304

[a]The column "bin size" provides the number of CCD lines that have been summed to constitute each spatial bin [see *Leblanc et al.*, 2006]. Solar Zenith Angle (SZA), Longitude, Latitude, Altitude (with a two km resolution) and Local time are for Mars Nearest Point of the FOV of the UV spectrograph. Ls is for areocentric longitude. F10.7 (10^{-22} W/m^2/Hz) are calculated from daily average National Geophysics Data Center taking into account the relative positions of the Earth and Mars, the Sun rotation and Mars' heliocentric distance.

identification of the (0,7) band at 293.6 nm because it is sandwiched between the strong CO_2^+ $B^2\Sigma^+ – X^2\Pi$ emission at 289.0 nm and the O emission at 297.2 nm. *Fox and Dalgarno* [1979] predicted that within the spectral range of SPICAM UVS the strongest emissions should be associated with the N_2 VK (0,5), (0,6) and (0,7) bands with intensities equal to 16, 20 and 20 Rayleigh (R) respectively. These authors also estimated overhead intensities of the emissions associated to the different bands of the Lyman-Birge-Hopfield $a^1\Pi_g – X^1\Sigma_g^+$ emission system which should not exceed 4 R. Whereas we clearly identified the (0,5) and (0,6) emission bands in SPICAM UVS spectra, we did not identify any of the emission bands of the Lyman-Birge-Hopfield $a^1\Pi_g – X^1\Sigma_g^+$ band system. The small intensity expected for these bands with respect to the SPICAM UVS sensitivity [*Bertaux et al.*, 2006] and the presence of numerous carbon, oxygen and CO emissions within the same spectral range may explain this non-detection.

[9] The 29 selected orbits include 57 limb viewing observations of the 120–170 km region in which 30 identifications of the VK (0,6) band and 28 identifications of the VK (0,5) band have been possible. Unfortunately it is difficult to extract for each individual orbit a clear dependence in altitude of the measured intensity. In the following part, we will discuss the measured intensity for each orbit when integrated between 120 and 170 km. Altitude profiles of the band emission are deduced from average spectra from the whole set of orbits within specific areocentric longitude and solar zenith angle ranges. The limb intensity of the VK (0,5) band integrated between 120 and 170 km varies between 109 and 456 R and is equal to 241 R on average. The intensity of the VK (0,6) band varies between 112 and 460 R with an average value of 223 R.

[10] The intensity of the VK (0,6) band can be compared to the intensity of the VK(0,5) band using the observations when both emissions are simultaneously identified (which occurs 21 times, see Figure 1). The best fit of the VK (0,6) and VK (0,5) ratio is:

$$\begin{aligned} 4\pi I_{0,6} &= (0.9 \pm 0.3) \times 4\pi I_{0.5} + (7 \pm 68) \text{ Rayleigh} \\ &\approx (0.9 \pm 0.3) \times 4\pi I_{0,5} \end{aligned} \tag{1}$$

These two emissions have therefore intensities very close to each other (7 R being less than 5% of the average measured intensity). *Fox and Dalgarno* [1979] have calculated a ratio for the intensities of these two emissions equal to 1.25 using transition probabilities and Franck-Condon factors. This result is in good agreement with the present measurement within its uncertainty.

[11] The variations of the intensities of the (0,6) and (0,5) bands with respect to the distance to the Sun should follow a law in $1/R^2$ with R Mars' heliocentric distance if the solar photon flux is the main driver for the production of these emissions. A best log-linear fit suggests a relation in $1/R^5$ but with an uncertainty on the power equal to ±19 suggesting that other sources of variability may be more important than the dependence on the heliocentric distance. The

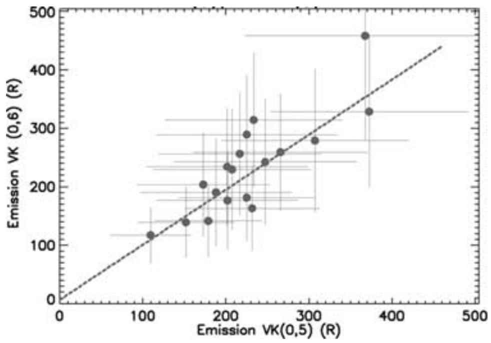

Figure 1. Emission intensity of the VK (0,5) band with respect to the emission intensity of the VK (0,6) band as extracted from average spectra obtained between 120 and 170 km in altitude (of the Mars Nearest Point of the light of sight). The best linear fit is VK(0,6)/VK(0,5) = 0.9 ± 0.3 (dashed line). Uncertainties on these values are deduced from the theoretical instrumental uncertainty [see *Leblanc et al.*, 2006].

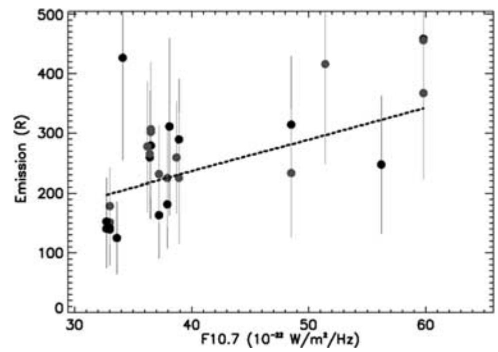

Figure 3. Emission intensities of the VK (0,5) band (grey dots) and (0,6) band (dark dots) with respect to the solar index F10.7 (10^{-22} W/m^2/Hz) measured at the Earth and extrapolated at Mars. The best fit (dashed line) corresponds to a law in (24 ± 52) + (5.3 ± 1.3) × F10.7. Average values of these intensities are calculated from spectra obtained between 120 and 170 km in altitude.

variation of the intensity of these two bands with respect to Solar Zenith Angle (SZA) is displayed in Figure 2. The best fit to the data displayed in Figure 2 corresponds to a variation of the intensity proportional to $\cos^{0.3\pm3}$(SZA). When analyzing the CO_2 emission dependence on SZA, *Leblanc et al.* [2006] reported a relation in cosine which provides a worse fit to the data in Figure 2. A potential discrepancy between the dependence of the Cameron CO_2 emission and of the N_2 VK (0,5) and (0,6) band emissions with respect to SZA may be related to the different origins of these two emissions: solar photons and photo-electrons, and the photo-electrons alone respectively.

[12] One important parameter that may change significantly the intensity of the observed emissions is the solar activity. Solar activity is usually represented by a solar activity index F10.7 which is the observed flux at 2800 Mhz (10.7 cm) in solar flux units (10^{-22} W/m^2/Hz) and calculated from daily average National Geophysics Data Center taking into account the relative positions of the Earth and Mars, the solar rotation and the heliocentric distance of Mars. Figure 3 displays the variation of the VK (0,6) and (0,5) bands emission intensities with respect to this index. The data set used in this paper covers a range of F10.7 index between 32.7 and 59.8 with an average value equal to 40.6 (that is for solar minimum conditions following *Bougher et al.* [2004]. The best fit, dashed line in Figure 3, corresponds to the following relation:

$$I_{VK}(\text{in Rayleigh}) = (24 \pm 52) + (5.3 \pm 1.3) \times \text{F10.7} \quad (2)$$

where I_{VK} is the limb viewing intensity of the VK band emission and F10.7 is the solar index at Mars.

[13] The profile of the intensity of the VK (0,6) emission is displayed in Figures 4c and 4d for two sets of areocentric longitude and 3 bins in solar zenith angle on each plot. In Figure 4c, a plateau or a small peak of the altitude profiles can be seen above 120 km. The measurements displayed in Figure 4d have been obtained with a significantly smaller data set and have therefore a much smaller signal/noise ratio than in Figure 4c. Below 120 km, the reported emissions do not decrease in altitude because of the difficulty of extracting properly these emissions from an increasing background due to diffuse light from the disk and from the dust layer. Figures 4a and 4d display the corresponding variation of the 289 nm emission. The 289 nm emission corresponds to the ultraviolet doublet 288.3–289.6 of the $B^2\Sigma_u^+ - X^2\Pi_g$ transition of the CO_2^+ ion [*Leblanc et al.*, 2006]. The main source for the production of this excited state has been identified as the photon and photo-electron impact and ionization of CO_2 [*Fox and Dalgarno*, 1979]. As a consequence, the intensity of this emission with respect to altitude can be directly associated with the variation of the CO_2 density if the region where it is measured is optically thin. *Leblanc et al.* [2006] have discussed the possibility of using the 289 nm emission rather than the brightest emission of the Martian UV dayglow, the Cameron band emission system between 190 and 270 nm, in order to derive upper atmospheric temperature. To derive such a temperature, we fit the intensity profile with a simple barometric law within a chosen altitude range (between 150 and 200 km in altitude in the present analysis). This fit provides a scale height from

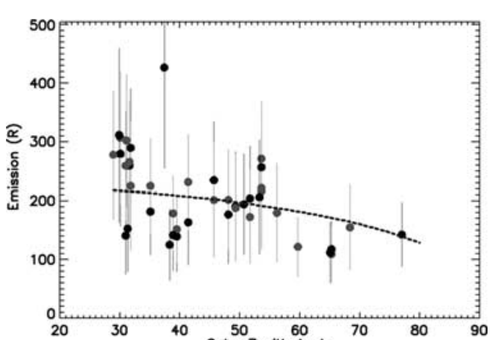

Figure 2. Emission intensities of the VK (0,5) band (grey dots) and (0,6) band (dark dots) with respect to the solar zenith angle from average spectra measured between 120 and 170 km in altitude (of Mars Nearest Point of the light of sight). The best fit (dashed line) corresponds to a law in $\text{cosine}^{(0.3\pm3)}$(SZA). Only observations obtained for minimum solar activity (F10.7 < 46) have been used.

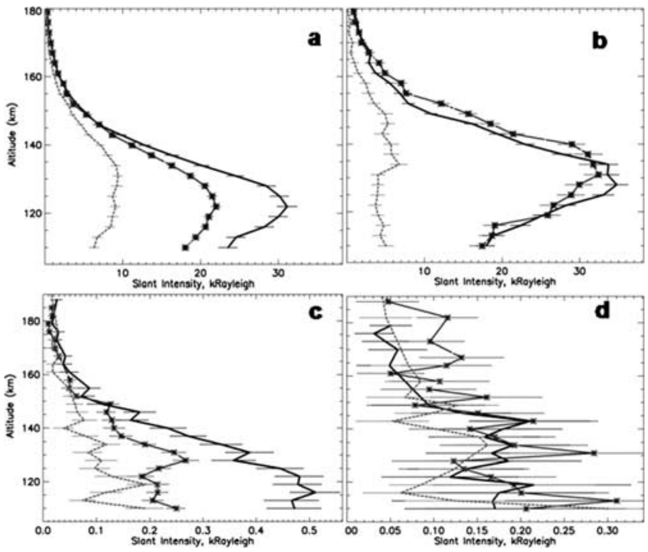

Figure 4. Average altitude profile (a, b) of the intensity of the emission at 289 nm and of the intensity (c, d) of the N_2 VK (0,6) band as calculated from average spectra using the full set of data (Table 1) and binned with respect to Mars areocentric longitude (Ls) and Solar Zenith Angle (SZA). Figures 4a and 4c are for Ls between 100° and 171° and Figures 4b and 4d are for Ls between 287° and 321°. Heavy line without symbols: SZA between 8° and 36°. Heavy line with stars: SZA between 36° and 64°. Light dashed line without symbols: SZA between 64° and 91°.

which the temperature can be calculated with the assumption that the main species leading to such an emission is CO_2 in the case of the 289 nm emission and N_2 in the case of the VK (0,6) band. The different temperatures derived by this method are displayed in Table 2.

[14] For the observations made between Ls = 100° and 171°, the average temperature of the CO_2 species is equal to 190 ± 7 K which is smaller than in the work by *Leblanc et al.* [2006] who found a value equal to 201 ± 10 K (the difference being due to the altitude range used in this paper as well as improvement of our understanding of the geometry of the observations). The average temperature derived from the analysis of the N_2 emission is equal to 190 ± 51 K which is therefore in good agreement with the temperature of the CO_2 species. For the observations made between Ls = 287° and 321°, the temperature for the CO_2 species is equal to 201 ± 13 K. The average temperature for the N_2 species is equal to 257 ± 71 K that is also in agreement with the corresponding CO_2 temperature. The altitude distribution of the N_2 and CO_2 species between 150 and 200 km is therefore in agreement with a diffusive separation regime. The CO_2 exospheric temperatures derived from SPICAM observations are significantly smaller than the temperatures predicted by the Mars Global Circulation Model of *Bougher et al.* [2000]. For Ls between 100 and 171° and solar minimum conditions, *Bougher et al.* [2000] predicted exospheric temperatures between 200 and 215 K, and for Ls above 280°, they predicted temperatures above 220 K. It is possible to roughly correct our measured profiles for the effect of the solar absorption with respect to solar zenith angle and altitude by using a theoretical CO_2 density profile [*Krasnopolsky*, 2002]. The results of this calculation is displayed in Table 2 between brackets. The average temperature derived from the 289 nm emission profile, after such a correction, is equal to 195 ± 7 K at Ls 100–171° and is equal to 207 ± 13 K at Ls 287–321°.

[15] The ratio of the path length of a limb viewing to the path length of nadir viewing can be used to estimate the ratio between the intensities of an emission measured with a limb viewing and of an emission measured with a nadir viewing as:

$$I_{Limb}/I_{Nadir} = \left(2 \times \Pi \times R_M/H\right)^{1/2} \quad (3)$$

where I_{Limb} and I_{Nadir} are for the integrated intensities of the emission with a limb and Nadir viewing respectively. R_M = 3395 km is the radius of Mars and H is the scale height of the N_2 species in the Martian upper atmosphere. From Figure 4, we can deduce the scale height of the N_2 species as being between 15 and 27 km with an average value equal to 19.5 ± 5 km. As a consequence, I_{Limb}/I_{Nadir} = 33. The Viking 1 conditions used by *Fox and Dalgarno* [1979] for their estimate of the intensity of this band correspond to a solar zenith angle of 45°, a solar index F10.7 equal to 29 and an atmospheric temperature of 200 K. For similar conditions of observation, SPICAM UVS measured a limb viewing intensity for the VK (0,6) band of ~180 R which should therefore correspond to a Nadir viewing intensity equal to 6 R. This value is therefore ~3 times smaller than the intensity calculated by *Fox and Dalgarno* [1979].

[16] The Mariner 6, 7 and 9 UV instruments did not detect the emissions associated with the N_2 VK bands. They associated a 270 nm spectral feature in the Mariner 9 data with the (1–5) CO^+ $B^2\Sigma^+–X^2\Sigma^+$ band [*Barth et al.*, 1971]. However a detailed analysis of Mariner 9 spectra did not confirm this identification [*Conway*, 1981]. The Mariner 6 and 7 measurements were carried out during high solar activity with a solar index F10.7 at Mars equal to 82 and 93 whereas Mariner 9 observations were done at solar index F10.7 equal to 38 and 48. Following equation (2), the

Table 2. Temperatures Derived From the Analysis of the Altitude Profiles of the Intensity of the 289 nm Emission and of the VK (0,6) Emission for Two Ranges of Areocentric Longitude and Three Solar Zenith Angle Ranges[a]

SZA, deg	T_{CO2}, K	T_{N2}, K
	LS 100°–171°	
8–36	195 (197) ± 7	181 ± 21
36–64	191 (195) ± 5	175 ± 79
64–91	185 (193) ± 9	214 ± 35
	LS 287°–321°	
8–36	201 (204) ± 5	193 ± 50
36–64	200 (203) ± 7	264 ± 64
64–91	203 (214) ± 21	313 ± 105

[a]T_{CO2} is 289 nm emission, T_{N2} is VK (0,6) emission, Ls is areocentric longitude, and SZA is solar zenith angle. The profiles for Ls between 100° and 171° have been derived using orbits between 947 and 1457 (21 orbits) whereas for Ls = 287° and 321° only 8 orbits were available. Values between brackets in the third column are temperatures calculated after correction of the measured profile by the effect of the solar absorption using the *Krasnopolsky* [2002] model of the CO_2 density.

intensity range of the N_2 VK (0,6) band emission that should have been observed by the Mariner 9 UV spectrometers should have been characterized by limb intensities between 120 and 400 R. In the same way, Mariner 6 and 7 should have observed limb viewing emission intensities between 300 and 690 R. *Dalgarno and McElroy* [1970] estimated that intensities with nadir geometry below 50 R (that is $\sim$1.5 kR with limb geometry) were below the threshold of detection of the Mariner missions. Therefore, the UV instruments on board Mariner 6, 7 and 9 missions were not able to detect the intensities measured by SPICAM UVS.

[17] There is a simple relation of proportionality between the mixing ratio and the nadir emission intensity for the brightest emission within the VK emission band system following *Dalgarno and McElroy* [1970]. These authors used such a relation to infer an upper limit for the mixing ratio of N_2 in the case of the non-detection of the VK emission by Mariner 6 UV instrument. Since the relation suggested by *Dalgarno and McElroy* [1970] was estimated for high solar activity, we used the result by *Fox and Dalgarno* [1979] at low solar activity Viking conditions to infer a new relation of proportionality between mixing ratio and overhead intensity. In the work by *Fox and Dalgarno* [1979], the overhead intensity of the (0,6) band is equal to 20 R for a mixing N_2/CO_2 ratio varying from 2.5% at the turbopause to $\sim$6% at 140 km and to 12% at 160 km [*Fox and Dalgarno*, 1979]. The overhead intensity of the VK emission should be related to the ratio of the column densities of N_2 and CO_2 in the region of the VK emission between 120 and 170 km (equivalent to a mixing ratio calculated for a uniformly mixed atmosphere as assumed by *Dalgarno and McElroy* [1970]). In the work by *Fox and Dalgarno* [1979], the 20 R overhead intensity of the VK (0,6) band corresponds to a ratio of the N_2/CO_2 column densities equal to $\sim$3% when integrated from 120 to 170 km in altitude. As a consequence, using the present measured emission of an overhead intensity of 6 R for similar conditions to Viking measurements, the ratio of the column densities of the N_2 and CO_2 between 120 and 170 km, that is the mixing ratio between N_2 and CO_2 for a uniformly mixed atmosphere, would be equal to 0.9%. Such a difference by a factor of $\sim$3 between the observed and calculated intensities is, most probably, partly or completely due to the updates in the molecular parameters of the photoelectron spectra, excitation cross sections, and quenching constants in the calculations of the VK bands by *Fox and Dalgarno* [1979], the smaller abundances of N_2 at 140 and 160 km in the recent models [*Krasnopolsky*, 2002], and the observational uncertainties of the VK band intensities.

4. Conclusions

[18] The dayglow emission associated with the electronic excitation of the N_2 Vegard-Kaplan band system has been identified for the first time by SPICAM UV spectrograph (UVS) on board Mars Express [*Leblanc et al.*, 2006]. In this paper, the main characteristics of this emission as deduced from the whole SPICAM set of observations are described. In particular, the overhead N_2 emission is shown to reach intensities between 5 and 15 R with small dependencies with respect to solar zenith angle and solar activity. This range of intensity is in agreement with the non-detection by Mariner 6, 7 and 9 UV spectrometers. A comparison between the observed intensities and the results obtained by *Fox and Dalgarno* [1979] in similar conditions than Viking 1 measurement suggest that these authors overestimated these emissions by a factor 3. The most likely explanation for this discrepancy is the fact that there are updated parameters from those used by *Fox and Dalgarno* [1979] as well as the uncertainties in the SPICAM UVS observations. Altitude profiles of the VK (0,6) band emission also suggest that the N_2 species is in diffusive separation regime in the Martian upper atmosphere (above 150 km).

[19] **Acknowledgments.** F.L. thanks O. Witasse and J. Lilensten for helpful comments. Mars Express is a space mission from ESA (European Space Agency).

References

Barth, C. A., W. G. Fastie, C. W. Hord, J. B. Pearce, K. K. Kelly, A. I. Stewart, G. E. Thomas, G. P. Anderson, and O. F. Raper (1969), Mariner 6: Ultraviolet spectrum of Mars upper atmosphere, *Science*, *165*, 1004–1005.

Barth, C. A., C. W. Hord, J. B. Pearce, K. K. Kelly, G. P. Anderson, and A. I. Stewart (1971), Mariner 6 and 7 Ultraviolet Spectrometer Experiment: Upper atmosphere data, *J. Geophys. Res.*, *76*, 2213–2227.

Bertaux, J.-L., et al. (2006), SPICAM on Mars Express: Observing modes and overview of UV spectrometer data and scientific results, *J. Geophys. Res.*, *111*, E10S90, doi:10.1029/2006JE002690.

Bougher, S. W., S. Engel, R. G. Roble, and B. Foster (2000), Comparative terrestrial planet thermospheres: 3. Solar cycle variation of global structure and winds at solstices, *J. Geophys. Res.*, *105*, 17,669–17,689.

Bougher, S. W., S. Engel, D. P. Hinson, and J. R. Murphy (2004), MGS Radio Science electron density profiles: Interannual variability and implications for the Martian neutral atmosphere, *J. Geophys. Res.*, *109*, E03010, doi:10.1029/2003JE002154.

Conway, R. R. (1981), Spectroscopy of the Cameron bands in the Mars airglow, *J. Geophys. Res.*, *86*, 4767–4775.

Dalgarno, A., and M. B. McElroy (1970), Mars: Is Nitrogen present?, *Science*, *170*, 167–168.

Dreyer, J. W., D. Perner, and C. R. Roy (1974), Rate constants for the quenching of $N_2(A^3\Sigma_u^+$, v_A = 0–8) by CO, CO_2, NH_3, NO and O_2, *J. Chem. Phys.*, *61*, 3164–3169.

Fox, J. L., and A. Dalgarno (1979), Ionization, luminosity, and heating of the upper atmosphere of Mars, *J. Geophys. Res.*, *84*, 7315–7333.

Fox, J. L., A. Dalgarno, E. R. Constantinides, and G. A. Victor (1977), The nitrogen dayglow on Mars, *J. Geophys. Res.*, *82*, 1615–1616.

Krasnopolsky, V. A. (2002), Mars' upper atmosphere and ionosphere at low, medium, and high solar activities: Implications for evolution of water, *J. Geophys. Res.*, *107*(E12), 5128, doi:10.1029/2001JE001809.

Leblanc, F., J. Y. Chaufray, J. Lilensten, O. Witasse, and J.-L. Bertaux (2006), Martian dayglow as seen by the SPICAM UV spectrograph on Mars Express, *J. Geophys. Res.*, *111*, E09S11, doi:10.1029/2005JE002664.

Meyer, J. A., D. W. Setser, and D. H. Stedman (1969), Excitation of the auroral green line of atomic oxygen ($^1S \rightarrow {}^1D$) by $N_2(A^3\Sigma_u^+)$, *Astrophys. J.*, *157*, 1023–1025.

Young, R. A., G. Black, and T. G. Slanger (1969), Vacuum-ultraviolet photolysis of N_2O. II. Deactivation of $N_2(A^3\Sigma_u^+)$ and $N_2(B^3\Pi_g)$, *J. Chem. Phys.*, *50*, 303–308.

J. L. Bertaux and J. Y. Chaufray, Service d'Aéronomie, Centre National de la Recherche Scientifique, Institut Pierre-Simon Laplace, F-91371, Verrières-le-Buisson, France.

F. Leblanc, Osservatorio Astronomico di Trieste, Via Tieppolo 11, I-34131, Trieste, Italy. (francois.leblanc@aerov.jussieu.fr)